



Generation of a High-Density Rat EST Map

Todd E. Scheetz, Michael R. Raymond, Darryl Y. Nishimura, et al.

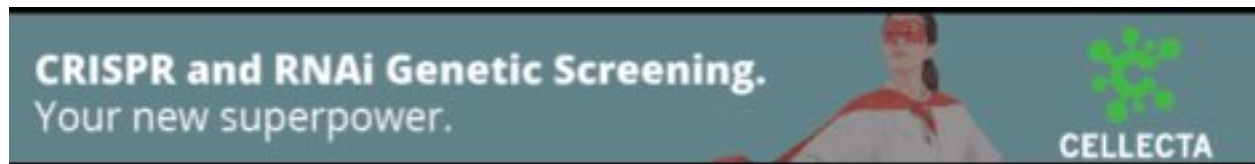
Genome Res. 2001 11: 497-502

Access the most recent version at doi:[10.1101/gr.151601](https://doi.org/10.1101/gr.151601)

License

Email Alerting Service

Receive free email alerts when new articles cite this article - sign up in the box at the top right corner of the article or [click here](#).



To subscribe to *Genome Research* go to:
<https://genome.cshlp.org/subscriptions>

Cold Spring Harbor Laboratory Press

Generation of a High-Density Rat EST Map

Todd E. Scheetz,^{1,2,3} Michael R. Raymond,^{1,2} Darryl Y. Nishimura,^{1,2}
Ann McClain,^{1,2} Chad Roberts,⁴ Clay Birkett,⁴ Jack Gardiner,⁵ Jie Zhang,^{1,2}
Nichole Butters,^{1,2} Christine Sun,^{1,2} Anne Kwitek-Black,⁶ Howard Jacob,⁶
Thomas L. Casavant,⁴ M. Bento Soares,^{2,3} and Val C. Sheffield,^{1,2,7}

¹Howard Hughes Medical Institute, ²Departments of Pediatrics, ³Physiology and Biophysics, and ⁴Electrical and Computer Engineering, University of Iowa, Iowa City, Iowa 52242, USA; ⁵Department of Agronomy, University of Missouri, Columbia, Missouri 65203, USA; ⁶Medical College of Wisconsin, Department of Physiology, Laboratory for Genetic Research, Milwaukee, Wisconsin 53226, USA

We have developed a high-density EST map of the rat, consisting of >11,000 ESTs. These ESTs were placed on a radiation hybrid framework map of genetic markers spanning all 20 rat autosomes, plus the X chromosome. The framework maps have a total size of ~12,400 cR, giving an average correspondence of 240 kb/cR. The frameworks are all LOD 3 chromosomal maps consisting of 775 radiation-hybrid-mapped genetic markers and ESTs. To date, we have generated radiation-hybrid-mapping data for >14,000 novel ESTs identified by our Rat Gene Discovery and Mapping Project (<http://ratEST.uiowa.edu>), from which we have placed >11,000 on our framework maps. To minimize mapping errors, ESTs were mapped in duplicate and consensus RH vectors produced for use in the placement procedure. This EST map was then used to construct high-density comparative maps between rat and human and rat and mouse. These maps will be a useful resource for positional cloning of genes for rat models of human diseases and in the creation and verification of a tiling set of map order for the upcoming rat-genome sequencing.

The rat provides excellent physiological and biochemical models for the study of genetically complex human disease, including hypertension (Hilbert et al. 1991; Jacob et al. 1991), renal disease (Brown et al. 1996), behavioral disorders (Moisan et al. 1996), and autoimmune disorders (Jacob et al. 1992). Given these rat models of human diseases, an increase in rat genomic resources will significantly benefit the study of human diseases. Such an increase in rat genomic information should also help in identifying the existence and function of the estimated 100,000 genes shared in mammals.

Although development of genomic resources for the rat initially lagged behind those available for mouse and human, in recent years several rat resources have been developed. Nearly 10,000 genetic markers have been identified, genetic framework maps have been generated (Steen et al. 1999; Watanabe et al. 1999), and first-generation human–rat and mouse–rat syntenic maps have been constructed (Watanabe et al. 1999). In addition, a radiation hybrid mapping panel (Rat T55) has been developed (Watanabe et al. 1999), and several thousand genetic markers have been mapped against this panel. Furthermore, >140,000 rat 3' ESTs have been generated (M.B. Soares, in prep.),

which have been used to define an NCBI UniGene (Schuler et al. 1997) set of >37,000 clusters and a local set of >51,000 distinct clusters (<http://ratEST.uiowa.edu/public/clustering/data/all.fasta.clus.html>). In this paper, we report the creation of two additional resources. The first is a placement map of >11,000 novel ESTs onto existing rat radiation hybrid framework maps and the construction of a consensus framework map consisting of 775 RH-mapped genetic markers and ESTs. These placement maps were essential resources for use in the construction of the second resource, high-resolution human–rat and mouse–rat syntenic maps, which in turn will be of benefit in identifying and classifying genes in both human and rat positional-cloning projects. The amount of gene discovery necessary to maintain a steady flow of novel ESTs to map is driven by the sequencing portion of the Rat Gene Discovery and Mapping Project at the University of Iowa (<http://ratEST.uiowa.edu>), which relies upon the technology of serial subtraction (Bonaldo et al. 1996) to minimize redundancy during gene discovery.

RESULTS

Generation of Genetic Framework Maps

The radiation hybrid framework was constructed primarily from publicly available mapping data, with a smaller amount of mapping data generated in our laboratory. All mapping data were generated using a subset of the T55 rat RH panel (Watanabe et al. 1999),

⁷Corresponding author.

E-MAIL val-sheffield@uiowa.edu; **FAX** 319-335-7588.

Article published on-line before print: *Genome Res.*, 10.1101/gr.151601.
Article and publication are at www.genome.org/cgi/doi/10.1101/gr.151601.

which was constructed with 3000 rads of X rays. The radiation hybrid framework maps developed in this study have an aggregate size of ~12,400 cR₃₀₀₀ and span all 20 rat autosomes and the X chromosome. Given that the total genome size of the rat is ~3000 Mb and 1500 cM (Steen et al. 1999), this framework has a correspondence of 240 kb/cR and 8.3 cR/cM, averaged across all chromosomes. Over 6000 unique, RH-mapped genetic markers were used in constructing our framework maps, of which 516 are actually utilized as framework markers. In addition, 259 ESTs were also incorporated to span large gaps from areas that were under-represented within the set of available RH-mapped genetic markers and to increase the overall density of the framework map. The availability of the large number of RH-mapped ESTs also helped in assembling the frameworks, especially in selecting only high-quality markers to incorporate into the framework. The frameworks are all LOD 3 frameworks with respect to permutations of local order, with an average distance between adjacent framework markers (i.e., the framework bin size) of 16.5 cR or ~4 Mb. A summary of framework statistics is provided in Table 1.

Placement of 11,000 Novel ESTs

To date, we have radiation-hybrid-retention data for >14,000 novel ESTs. The average retention rate of our RH-mapped ESTs was found to be 29.1%, with a discordancy rate of 3.7%. This is comparable with the quoted 27% retention rate of the T55v3 panel (Watanabe et al. 1999). The average retention rate over all of

the RH-mapped genetic markers was 26.7%. Of the 14,000 RH-mapped ESTs, >11,000 place onto the Iowa radiation hybrid framework, yielding an average density of 3.7 mapped ESTs per Megabase. Overall, 11,100 ESTs were placed onto the Iowa framework maps, of which 10,801 placed uniquely. Of these 10,801 placements, 3989 were of LOD 3 or better versus other potential placements, with nearly all of the remaining placements due to placement adjacent to a framework marker. Markers that place adjacent to framework markers often exhibit equivalent placement on either side of the framework marker, thereby exhibiting reduced LODs, although still providing an accurate localization. Similarly, a total of 11,064 ESTs placed on the Oxford framework maps and 11,386 ESTs placed on the Medical College of Wisconsin (MCW) maps. A total of 12,674 ESTs can be placed—11,512 uniquely—on at least one of the three framework maps. A comparison of EST placements on the three framework maps is shown in Table 2. A summary of EST placements on the VI framework maps compared to the combination of all framework maps is shown in Table 3. The additional placement of ESTs across all frameworks serves as an indicator of regions that may benefit from further improvement in framework maps. Additional updates to the framework maps should allow many of these ESTs to place without relaxing the placement stringency. Those ESTs that don't place on any map also will be analyzed further to determine the cause of their failure to place. As a verification of our RH EST placement map, we compared the localization

Table 1. Summary of Framework Statistics

Chromosome	Size (Mb)	Size (cM)	Size (cR)	kb/cR	cR/cM	No. of framework markers	Avg. bin size (cR)
Total	3001	1503	12441	241.2	8.28	775	16.5
1	301	141	1191	252.7	8.45	90	13.4
2	268	111	618	433.7	5.56	45	14.0
3	203	94	440	461.4	4.68	35	12.9
4	198	104	553	358.0	5.31	35	16.3
5	181	98	536	337.7	5.47	40	13.7
6	158	73	629	251.2	8.62	47	13.7
7	153	79	657	232.9	8.32	39	17.3
8	142	84	811	175.1	9.65	54	15.3
9	135	79	612	220.6	7.75	39	16.1
10	128	93	1060	120.8	11.40	67	16.1
11	110	49	348	316.1	7.10	20	18.3
12	76	43	379	200.5	8.81	24	16.5
13	118	46	460	256.5	10.00	23	20.9
14	116	69	766	151.4	11.10	39	20.2
15	111	69	622	178.5	9.01	35	18.3
16	101	46	461	219.1	10.02	26	18.4
17	100	50	434	230.4	8.68	26	17.4
18	95	52	547	173.7	10.52	26	21.9
19	77	44	455	169.2	10.34	24	19.8
20	67	37	521	128.6	14.08	22	24.8
X	163	42	341	478.0	8.12	19	19.0

of ESTs in our placement map with the genetically determined location of genes, as annotated in NCBI's UniGene set. Overall, of 111 genes that had both RH-mapped ESTs and genetic mapping data available, the localization of 104 (94%) was the same. Of the seven ESTs with discordant localization, one was determined to be correctly mapped based on annotated location in both LocusLink and RATMAP. Three others appear likely to have correct localization based on the human-rat conserved segments published in Watanabe et al. (1999) and those presented in this paper. For the remaining three ESTs that exhibited discordant localization in this analysis, there is not sufficient data to draw a conclusion; however, potential sources of error include either mapping source (our EST maps or that included in the UniGene annotation) and the BLAST based method for identifying the EST to gene relationship.

Duplicate vs. Single-Scored RH Vectors

To minimize errors, we generated independent duplicate mapping data for each EST; however, duplicate mapping adds significantly to the cost of radiation hybrid mapping. To quantitatively evaluate the benefit of duplicate mapping versus single mapping, the following analysis was performed on a set of 7856 placed ESTs. Both scores used to generate the consensus RH vector (as described in Methods) were placed against our framework maps and the resulting placements compared to that of the consensus RH vectors. Overall, the single-scored RH vectors placed in the same bin as the consensus RH vector with a high degree of reliability. Specifically, for 7463 (95%) both single-scored RH vectors placed in the same bin or adjacent bin as the consensus vector, with 75% identical placement to the consensus vector. Therefore, duplicate mapping helped identify and fix problematic mapping.

Comparative Maps

Utilizing the EST placement maps described above, comparative maps were constructed using a BLAST-based method to identify potential orthologs. A total of 190 rat-human and 145 rat-mouse conserved segments were identified, requiring at least two potential orthologs that colocalize in both species to define a conserved segment. Most of the previously identified

rat-human conserved segments (Watanabe et al. 1999) were identified in these maps; however, many of the previously identified smaller rat-mouse segments were not identified in this analysis, most likely due to the relatively limited number of RH-mapped mouse ESTs as compared to RH-mapped human sequences. Of the 190 rat-human segments identified, 25 are novel (not previously described), whereas in the mouse, only five novel conserved segments were identified. As expected, multiple complex rearrangements were noted within the longer conserved segments.

DISCUSSION

Comparison to Existing Framework Maps

At least two other RH framework maps have been produced to date by groups at Oxford (Watanabe et al. 1999) and MCW (Steen et al. 1999). Our Iowa framework maps are consistently smaller than either the MCW or Oxford maps (Fig. 1); however, they place ESTs as well as either map. A summary of framework size and EST placement is given for all three sets of maps in Table 2. This difference in size is most likely due to exclusion of markers that expanded map size in our framework map, compared to the larger number of markers in the Oxford and MCW maps. Integration of markers with errors can cause map expansion both by increasing the number of apparent breaks and by decreasing the linkage between markers through an increased number of ambiguities in retention. Such markers are most likely integrated due to an insufficient number of RH vectors in certain regions of the rat genome when the frameworks were constructed. To aid in unifying the MCW and Oxford maps, we generated scaffold maps with the framework markers from the Oxford and MCW maps placed upon the Iowa framework maps.

Syntenic Segments

Most of the previously identified conserved syntenic segments between rat and human, and rat and mouse, were verified using our EST placement map. In addition, many new segments were identified, predominantly in the rat-human maps. One of the largest differences between the comparative maps reported here and those in Watanabe et al. (1999) are in the distal-most region of the q-arm of RNO6. Specifically, Watanabe et al. (1999) identified several conserved segments broadly conserved regions to human 14q and two smaller conserved segments to human 6q21-22.2 and 6q22.3-6q24. These smaller 6q regions are not present in our rat-human comparative map nor are they present in the corresponding segments to mouse chromosome 10 in the rat-mouse comparative map. These differences are most likely due to fail-

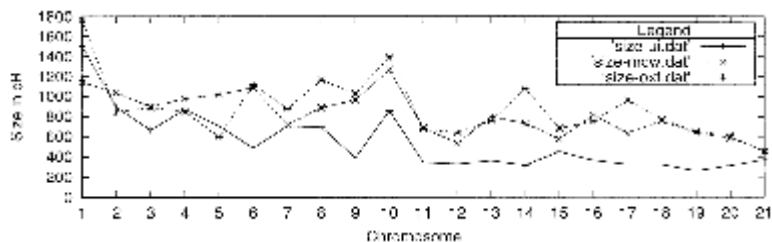


Figure 1 Comparison of framework sizes.

Table 2. Comparison of Frameworks

Chromosome	Size (cR) UI	Size (cR) WCW	Size (cR) Oxford	No. placed UI	No. placed MCW	No. placed Oxford
All	12441	17199	18555	11100	11386	11064
1	1191	1144	1762	1505	1464	1556
2	618	1037	845	893	932	902
3	440	898	889	663	778	699
4	553	977	850	870	953	769
5	536	1020	594	705	857	658
6	629	1086	1121	484	567	581
7	657	716	876	703	683	647
8	811	887	1164	692	755	872
9	612	965	1031	388	443	440
10	1060	1266	1399	856	948	960
11	348	685	675	344	348	327
12	379	532	637	328	351	312
13	460	799	757	359	364	411
14	766	730	1078	316	308	359
15	622	576	681	450	340	295
16	461	815	753	363	358	323
17	434	631	963	324	328	368
18	547	755	766	321	342	315
19	455	635	653	264	301	195
20	521	588	610	312	320	300
X	341	458	450	370	247	153

ure to fully cap the University of Iowa chromosome 6 framework map. This example illustrates the utility of having multiple sets of data that can be used to identify areas where further work may be required and/or beneficial.

Most of the complex rearrangements identified were found in the human, which is to be expected for two reasons. The first is artifactual: Given significantly more placed ESTs and genes in the human, it is easier to find the subtle differences that denote rearrange-

Table 3. Summary of EST Placement

Chromosome	UI frameworks		All frameworks	
	Placement	Unique placement	Placement	Unique placement
Total	11100	10801	12674	11512
1	1505	1444	1766	1426
2	893	774	1169	655
3	663	623	945	764
4	870	730	1121	686
5	705	633	953	698
6	484	480	623	605
7	703	693	769	715
8	692	679	1007	739
9	388	384	527	484
10	856	820	1095	876
11	344	306	447	323
12	328	326	377	359
13	359	358	442	431
14	316	313	412	386
15	450	400	510	406
16	363	352	414	387
17	324	321	400	389
18	321	315	369	355
19	264	262	325	278
20	312	312	353	337
X	370	276	397	213

ments. The second is phylogenetic: Given the increased evolutionary distance between human and rat compared to that between mouse and rat, the quantity of rearrangements would be expected to be higher, leading to more frequent complex rearrangements.

We have described the construction of a radiation hybrid framework map built from genetic markers upon which we have placed >11,000 novel RH-mapped ESTs and high-density human–rat and mouse–rat comparative maps. The development of an EST placement map is only the first step in developing important resources to further other avenues of research. Future work in this area includes mapping of additional rat ESTs, continued addition to and refinement of the human–rat and mouse–rat comparative maps, and integration of the comparative maps into our database and our Web site (<http://ratEST.uiowa.edu>). Such maps will be a valuable resource to traditional human-disease-oriented efforts, allowing the use of rat models of human disease to the fullest extent.

METHODS

Selection of ESTs for Mapping

Only one member from each novel cluster was chosen from a clustering of >140,000 3' reads. It is significant that 3 reads are used, so that the end of the original mRNA can be reliably captured using poly-A capturing techniques. Selection of only one member from each cluster helps ensure that each gene is mapped only once. We preferentially selected clusters for mapping with an identifiable poly-A tail to help ensure an anchored 3'-end read. Primers were then chosen using Primer 3.0 (http://www-genome.wi.mit.edu/genome_software/other/ptimer3.html) and synthesized using phosphoamidite chemistry by Research Genetics.

Primer Testing

Primer pairs were tested to verify rat-specific amplification prior to radiation hybrid mapping against the complete T55v2 panel. Testing was carried out at two different annealing temperatures (60°C and 62°C) using the same PCR protocol used for radiation hybrid mapping (see below). Primer pairs that amplified a discrete rat band in the absence of a hamster band were used for RH mapping. If a primer pair amplified a weak hamster band at either temperature, it was retested with annealing temperatures of 62°C and 64°C. If a primer pair did not amplify at 60°C or 62°C, it was retested with an annealing temperature of 59°C and a 1-min extension time. Only primer pairs giving a discrete rat band in the absence of a hamster band for at least one annealing temperature were mapped against the RH panel.

Radiation Hybrid Mapping

To minimize errors in the radiation hybrid data vectors produced, EST-derived radiation-hybrid-mapping data were generated in duplicate. This allowed a consensus vector to be constructed. Primer pairs were amplified using a modified Touchdown PCR protocol (Don et al. 1991), in which the first five rounds of amplification start with an annealing temperature 5°C higher than the specified annealing temperature, as

determined in the testing procedure, dropping 1°C at each iteration. After the first five rounds, 35 more rounds of amplification are carried out with a melting temperature of 95°C, annealing temperature as determined by the testing procedure, and an extension temperature of 72°C. Each duplicate reaction is performed using aliquots from the same master mix to minimize variation. The PCR amplification is carried out on the T55 hybrid panel. Specifically, 94 hybrids from the original 106 are used, which has been denoted as the T55v2 panel (Watanabe et al. 1999). The resulting PCR products are then electrophoresed on a 2% agarose gel with ethidium bromide (1 µL/100 mL) for 30 min at 200 volts and imaged with a Mitsubishi P90 camera using a C.B.S. Scientific.

RH data were scored from the gel image using a custom computer-based scoring tool, *RHSCORER* (<http://ratEST.uiowa.edu/pubsoft/software.html> UV-illumination source), for the presence (1) or absence (0) of a band. An ambiguous score (2) was assigned when the retention was indeterminate (e.g., when a dim band was visible). *RHSCORER* allows digital images of the mapping gels to be loaded and scored with each lane's score clearly visible, thus limiting the amount of errors introduced by data transcription or entry. More recent versions of *RHSCORER* allow correction of skew due to imperfect alignment of the gel when imaged, reducing the amount of discordance between duplicate typings. Consensus RH vectors were constructed by requiring concordance for a given hybrid in both single-scored RH vectors, discordant positions were assigned an ambiguous score (2). Discordant RH vectors were not used in the placement.

Framework Construction and EST Placement

The chromosomal framework maps on which all of our ESTs are placed are anchored to existing genetic maps (Steen et al. 1999) through the use of 516 genetic markers. These genetic markers are from a pool of more than 6000 unique genetic markers, including those mapped locally and those for which RH-vector data are publicly available (Steen et al. 1999; Watanabe et al. 1999) from RHdb (Rodriguez-Tomé and Lijnzaad 1997; <http://www.ebi.ac.uk/RHdb/>).

Construction of the maps was performed using the *RHMAPPER* package (<http://www.genome.wi.mit.edu/ftp/pub/software/rhmapper>). When possible, automated techniques were developed and used to reduce the amount of user interaction required during framework construction. However, all maps, regardless of the methods used in construction, were verified to ensure that only high-quality markers were used in the construction of the framework map. Two criteria were used for evaluating marker quality: (1) the number of discordant scores (2s) present in the RH vectors and (2) the presence of highly similar RH vectors in the data set (either genetic markers or ESTs). RH vectors with large numbers of discordant scores exhibit reduced linkage, which leads to map expansion and improper linkage to distant markers, making accurate localization difficult. By requiring the presence of highly similar data vectors, we minimized the possibility of incorporating a mis-scored marker into our framework, which would otherwise degrade the quality of the maps. Through the use of these quality criteria, we were able to restrict the markers in our framework maps to those that exhibited the highest quality.

Framework construction proceeded in multiple phases, beginning with construction of small (subchromosomal) contiguous segments. This was done without reference to genetic maps, both to avoid any bias and to provide independent verification of marker order. During the second phase the

segments were assembled, which necessitated spanning some large and/or ambiguous gaps. The genetic maps were exploited when spanning particularly difficult gaps to identify potential markers within a particular region. During the third phase, the framework maps were capped by verifying the use of the most telomeric markers available, and medium to large (>20 cR) gaps were filled when possible. The fourth phase of framework construction consisted of reevaluating individual chromosome framework maps to verify that only high quality markers were used. The final step in the framework construction was an attempt to increase the framework density through incorporation of EST as framework markers.

The EST placement map was created using the CREATE_PLACEMENT_MAP function of RHMAPPER using the consensus RH vectors. All ESTs for which RH data were generated were placed upon our maps unless either (1) retention was 0%, or (2) discordancy was present in 14 or more of the 94 hybrids. Three consecutive placement attempts were run to maximize unique placements. In the first pass, default parameters were used except for a value of 15.0 for PLACEMENT_LINKAGE. This allowed those ESTs most tightly linked to the framework markers to place. In the second pass, the PLACEMENT_LINKAGE constraint was reduced to 10.0. For the final pass of placement, a value of 20 for the PLACEMENT_TOO_FAR parameter was used to attempt placement of ESTs not placed in the first two passes. Relaxing these parameters allowed ESTs to place within the larger bins. Further relaxation of these parameters allowed more ESTs to place but resulted in significantly higher rates of multiple (i.e., nonunique) placement. Additional updates to the framework maps should allow many of the remaining ESTs to place without relaxing the placement stringency.

Methods Used in External Mapping Verification

Mapped EST sequences were BLASTed against NCBI's rat UniGene set, and the chromosomal localization, as annotated with the CYTOBAND tag, of each hit was compared to the localization from our EST placement map. Only ESTs whose 3' and 5' sequences both hit the same UniGene cluster above a BLAST *E*-value of 1e-45 were used in this analysis.

Comparative Map Construction

A BLAST-based method was used to identify potential orthologs, utilizing a relatively low bit-score cutoff of 100. Although less strict than the method used by Watanabe et al. (1999), based upon published results (Makalowski and Boguski 1998a,b) such a criteria provide a good indication of potential orthologs. The ePCR results from GeneMap (Deloukas et al. 1998) were used to identify locations of human ESTs and genes. Similar localization data for the mouse was obtained from the mouse RH home page (http://www-genome.wi.mit.edu/mouse_rh/index.html). Each RH-mapped rat EST sequence was blasted against both dbEST and the nonredundant nucleotide database. A set of programs was designed to utilize these files, along with the EST placement data and the BLAST results, to create files listing the rat-human and rat-mouse comparative maps with all potential orthologs shown. These files were then used to identify conserved segments, using the criteria that at least two markers colocalize across species.

ACKNOWLEDGMENTS

We thank N. Altman, M. Anderson, J. Assouline, N. Bedford,

B. Berger, R. Brown, K. Crouch, M. Donohue, G. Doonan, B. Johnson, R. Kinkaid, S. Mackerley, E. Mallett, V. Miljkovic, B. Rhoads, C. Smith, and H. Young for technical assistance; T.A. Kucaba for supervision and coordination of the EST sequencing; and Michael James for early access to radiation hybrid data on genetic markers. This work was supported in part by NIH grant 2R01HL59789. T.E.S. is partially supported by a NIH training grant. V.C.S. is an Associate Investigator of the Howard Hughes Medical Institute.

The publication costs of this article were defrayed in part by payment of page charges. This article must therefore be hereby marked "advertisement" in accordance with 18 USC section 1734 solely to indicate this fact.

REFERENCES

- Bonaldo, M.F., Lennon, G., and Soares, M.B. 1996. Normalization and subtraction: Two approaches to facilitate gene discovery. *Genome Res.* **6**: 791–806.
- Brown, D.M., Provost, A.P., Daly, M.J., Lander, E.S., and Jacob, H.J. 1996. Renal disease susceptibility and hypertension are under independent genetic control in the fawn-hooded rat. *Nat. Genet.* **12**: 44–51.
- Deloukas, P., Schuler, G.D., Gyapay, G., Beasley, E.M., Soderlund, C., Rodriguez-Tomé, P., Hui, L., Matisse, T.C., McKusiak, K.B., Beckmann, J.S., et al. 1998. A physical map of 30,000 human genes. *Science* **282**: 744–746.
- Don, R.H., Cox, P.T., Wainwright, B.J., Baker, K., and Mattick, J.S. 1991. 'Touchdown' PCR to circumvent spurious priming during gene amplification. *Nucleic Acids Res.* **19**: 4008.
- Hilbert, P., Lindpaintner, K., Beckmann, J.S., Serikawa, T., Soubrier, F., Dubay, C., Cartwright, P., Degouyon, B., Julier, C., Takahashi, S., et al. 1991. Chromosomal mapping of two genetic loci associated with blood-pressure regulation in hereditary hypertensive rats. *Nature* **353**: 521–529.
- Jacob, H.J., Lindpaintner, K., Lincoln, S.E., Kusumi, K., Bunker, R.K., Mao, Y.P., Ganten, D., Dzau, V.J., Lander, E.S. 1991. Genetic mapping of a major gene causing hypertension in the stroke-prone spontaneously hypertensive rat. *Cell* **67**: 213–224.
- Jacob, H.J., Petterson, A., Wilson, D., Mao, Y., Lemark, A., Lander, E.S. 1992. Genetic dissection of autoimmune type I diabetes in the BB rat. *Nat. Genet.* **2**: 56–60.
- Makalowski, W. and Boguski, M.S. 1998a. Evolutionary parameters of the transcribed mammalian genome: An analysis of 2,820 orthologous rodent and human sequences. *Proc. Natl. Acad. Sci.* **95**: 9407–9412.
- . 1998b. Synonymous and nonsynonymous substitution distances are correlated in mouse and rat genes. *J. Mol. Evol.* **47**: 119–121.
- Moisan, M-P., Courvoisier, H., Bihoreau, M.T., Gaugier, D., Hendley, E.D., Lathrop, M., James, M.R., Mormede, P. 1996. A major quantitative trait locus influences hyperactivity in the rat. *Nat. Genet.* **14**: 471–473.
- Rodriguez-Tomé, P. and Lijnzaad, P. 1997. The Radiation Hybrid Database. *Nucleic Acids Res.* **25**: 81–84.
- Schuler, G.D. 1997. Pieces of the puzzle: Expressed sequence tags and the catalog of human genes. *J. Mol. Med.* **75**: 694–698.
- Steen, R.G., Kwitek-Black, A.E., Glenn, C., Guillings-Handley, J., Van Etten, W., Atkinson, O.S., Appel, D., Twigger, S., Muir, M., Mull, T., et al. 1999. A high density integrated genetic and radiation hybrid map of the laboratory rat. *Genome Res.* **9**: AP1–8.
- Watanabe, T.K., Bihoreau, M.T., McCarthy, L.C., Kiguwa, S.L., Hishigaki, H., Tsuji, A., Browne, J., Yamasaki, Y., Mizoguchi-Miyakita, A., Oga, K., et al. 1999. A radiation hybrid map of the rat genome containing 5,255 markers. *Nat. Genet.* **22**: 27–36.

Received June 8, 2000; accepted in revised form December 8, 2000.